Hybrid high-order (HHO) method for modeling and numerical simulation of seismic-acoustic wave propagation

Author : Romain Mottier[§††] (PhD student) **Supervision** : Alexandre Ern [†‡], Laurent Guillot[§]

[§] French Alternative Energies and Atomic Energy Commission (CEA)
[†] Teaching and Research Center in Mathematics and Scientific Computing (CERMICS)
[‡] French Institute for Research in Numerical Science and Technology (INRIA - SERENA TEAM)

Context and issues

Objectives

- Accurate modelisation and simulation of seismo-acoustic waves **through heterogeneous domains with complex geometries**
- Treatment of realistic cases of interest
  - ► High Performance Computing (HPC)

Issues

- Difficulty to mesh complex geometries
- High-order precision needed to accurately capture waves
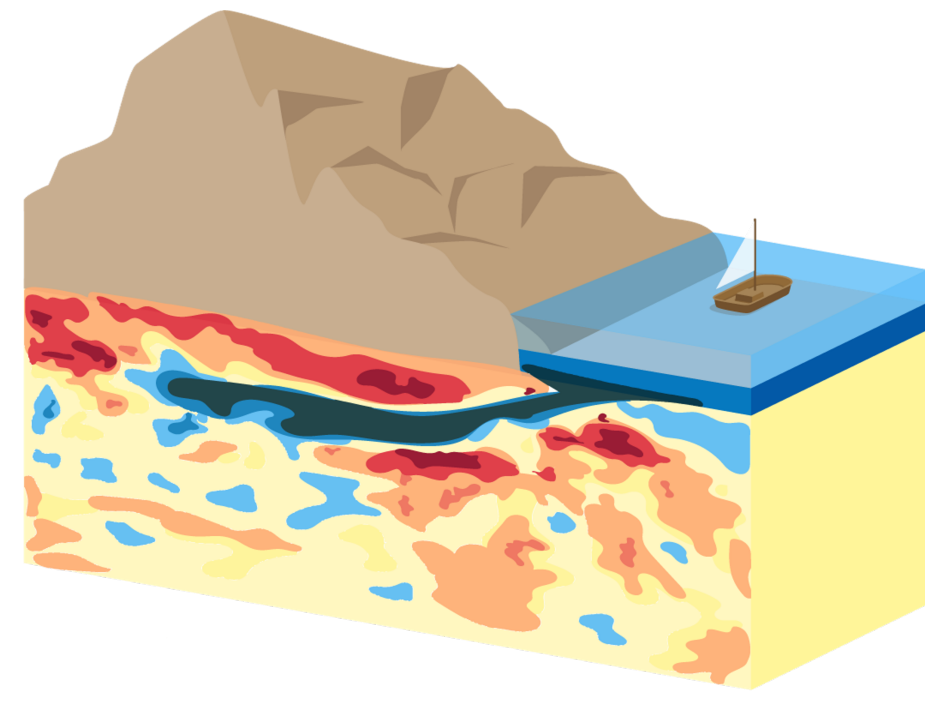 - ► Hybrid discontinuous methods (HDG/HHO)

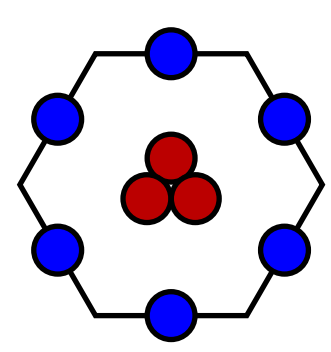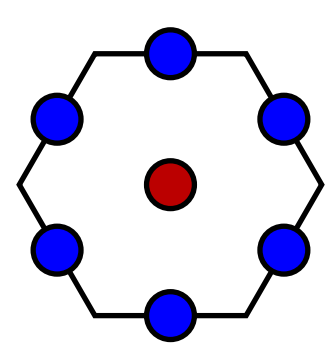

Fig. 1: Lateral heterogeneities near the earth's surface.

Coupling of the acoustic and elastic wave equations

- **Elastic wave equation:**
$$\begin{cases} \partial_t \varepsilon(t) - \nabla^s v(t) = \mathbf{0} \\ \rho_S \partial_t v(t) - \nabla \cdot (\mathcal{C} : \varepsilon(t)) = f(t) \end{cases}$$

- **Acoustic wave equation:**
$$\begin{cases} \frac{1}{\kappa} \partial_t p(t) + \nabla \cdot v(t) = g \\ \rho_F \partial_t v(t) + \nabla p(t) = \mathbf{0} \end{cases}$$

- **Coupling condition:**
$$\begin{cases} [\![v(t) \cdot n_\Gamma]\!]_\Gamma = 0 \\ (\mathcal{C} : \varepsilon(t)) \cdot n_\Gamma = p(t) n_\Gamma \end{cases}$$

The HHO method

Degrees of freedom

- **Principle:** Polynomial unknowns located in the cells and on the faces

HHO unknowns:
$$\hat{u}_h := (u_{\mathcal{T}}, u_{\mathcal{F}})$$

● Cell unknowns of degree k' ● Face unknowns of degree k

Fig. 2: Left panel: Equal-order discretization ($k' = k = 0$). Right panel: Mixed-order discretization ($k' = k + 1 = 1$).

Operators

- **Gradient reconstruction operator:** $\nabla u \to G(\hat{u}_h)$
- **Stabilization operator:** $s(\hat{u}_h, \hat{w}_h)$
  - ► Penalization at the element level to ensure stability while preserving the approximation properties of the reconstruction.

Advantages

- **Mesh flexibility:**
  - ► Complex geometries
  - ► Unstructured and polyhedral meshes
  - ► Local mesh refinement
- **Local conservativity**

- **Optimal error estimates for smooth solutions**
- **Attractive computational costs:**
  - ► Global problem couples only face dofs
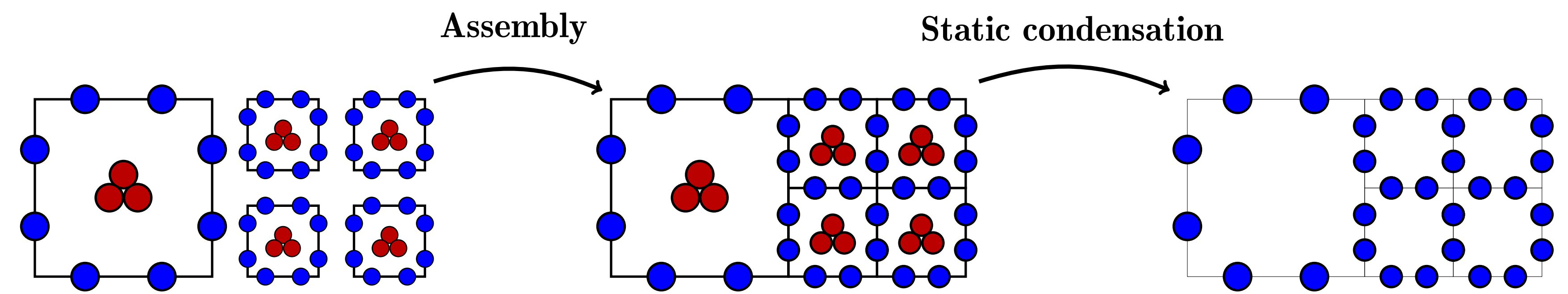 - ► Cell dofs recovered by local post-processing

Assembly   **Static condensation**

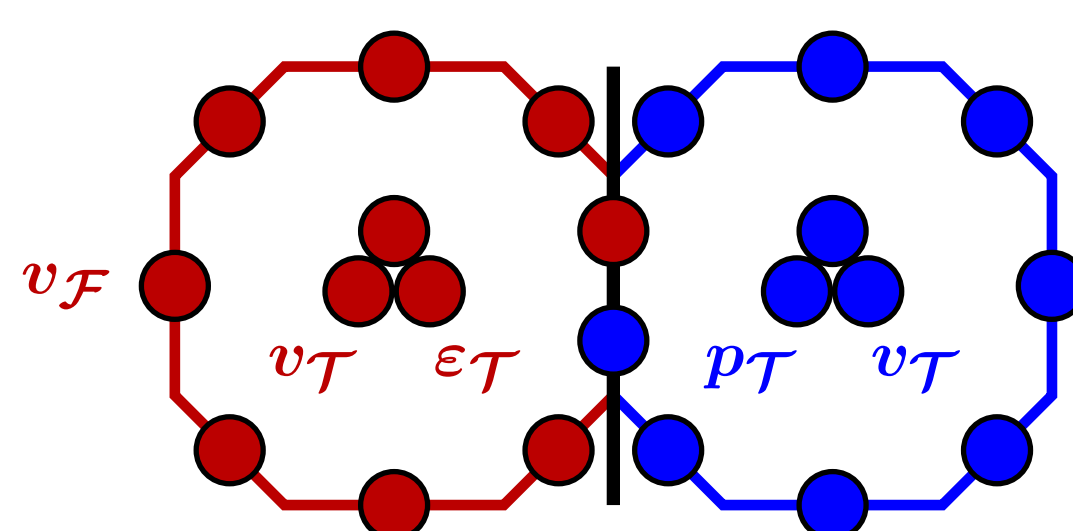Fig. 3: Static condensation procedure.

HHO space semi-discretization

- **Approximation spaces:**
  - ► **Fluid domain:**
$$V_{\mathcal{T}_F}^k := \bigtimes_{T \in \mathcal{T}_h^F} \mathbb{P}^k(T; \mathbb{R}^d), \qquad \hat{V}_h^F := \bigtimes_{T \in \mathcal{T}_h^F} \mathbb{P}^{k'}(T; \mathbb{R}) \times \bigtimes_{F \in \mathcal{F}_h^F} \mathbb{P}^k(F; \mathbb{R})$$
  - ► **Elastic domain:**
$$\mathcal{Z}_{\mathcal{T}_S}^k := \bigtimes_{T \in \mathcal{T}_h^S} \mathbb{P}^k(T; \mathbb{R}_{\text{sym}}^{d \times d}), \quad \hat{V}_h^S := \bigtimes_{T \in \mathcal{T}_h^S} \mathbb{P}^{k'}(T; \mathbb{R}^d) \times \bigtimes_{F \in \mathcal{F}_h^S} \mathbb{P}^k(F; \mathbb{R}^d)$$

Fig. 4: Elasto-acoustic unknowns with a mixed-order ($k' = k + 1 = 1$) discretization.

- **Elasto-acoustic coupling:**
$$\begin{cases} (\partial_t v_{\mathcal{T}}^F(t), r_{\mathcal{T}})_{L^2(\rho_F; \Omega_F)} + (G_{\mathcal{T}}(\hat{p}_h(t)), r_{\mathcal{T}})_{L^2(\Omega_F)} = 0 \\ (\partial_t p_{\mathcal{T}}(t), q_{\mathcal{T}})_{L^2(\frac{1}{\kappa}; \Omega_F)} - (v_{\mathcal{T}}^F(t), G_{\mathcal{T}}(\hat{q}_h))_{L^2(\Omega_F)} + s_h^F(\hat{p}_h(t), \hat{q}_h) - (v_{\mathcal{F}}^S(t) \cdot n_\Gamma, q_{\mathcal{F}})_{L^2(\Gamma)} = (g(t), q_{\mathcal{T}})_{L^2(\Omega_F)} \\ (\partial_t \varepsilon_{\mathcal{T}}(t), z_{\mathcal{T}})_{L^2(\Omega_S)} - (E_{\mathcal{T}}(\hat{v}_h(t)), z_{\mathcal{T}})_{L^2(\Omega_S)} = 0 \\ (\partial_t v_{\mathcal{T}}(t), w_{\mathcal{T}})_{L^2(\rho; \Omega_S)} + (\varepsilon_{\mathcal{T}}, E_{\mathcal{T}}(\hat{w}_h))_{L^2(\mathcal{C}; \Omega_S)} + s_h^S(\hat{v}_h^S(t), \hat{w}_h) + (p_{\mathcal{F}}(t), w_{\mathcal{F}} \cdot n_\Gamma)_{L^2(\Gamma)} = (f(t), w_{\mathcal{T}})_{L^2(\Omega_S)} \end{cases}$$

- **Algebraic realization:**

$$\begin{bmatrix} M_{\mathcal{T}\mathcal{T}}^v & 0 & 0 & 0 & 0 & 0 \\ 0 & M_{\mathcal{T}\mathcal{T}}^F & 0 & 0 & 0 & 0 \\ 0 & 0 & 0 & 0 & 0 & 0 \\ 0 & 0 & 0 & M_{\mathcal{T}\mathcal{T}}^\varepsilon & 0 & 0 \\ 0 & 0 & 0 & 0 & M_{\mathcal{T}\mathcal{T}}^S & 0 \\ 0 & 0 & 0 & 0 & 0 & 0 \end{bmatrix} \begin{bmatrix} \partial_t V_{\mathcal{T}}^F \\ \partial_t P_{\mathcal{T}} \\ \partial_t P_{\mathcal{F}} \\ \partial_t S_{\mathcal{T}} \\ \partial_t V_{\mathcal{T}} \\ \partial_t V_{\mathcal{F}} \end{bmatrix} + \begin{bmatrix} 0 & -G_{\mathcal{T}} & -G_{\mathcal{F}} & 0 & 0 & 0 \\ G_{\mathcal{T}}^\dagger & \Sigma_{\mathcal{T}\mathcal{T}}^F & \Sigma_{\mathcal{T}\mathcal{F}}^F & 0 & 0 & 0 \\ G_{\mathcal{F}}^\dagger & \Sigma_{\mathcal{F}\mathcal{T}}^F & \Sigma_{\mathcal{F}\mathcal{F}}^F & 0 & 0 & C_\Gamma \\ 0 & 0 & 0 & 0 & -E_{\mathcal{T}} & -E_{\mathcal{F}} \\ 0 & 0 & 0 & E_{\mathcal{T}}^\dagger & \Sigma_{\mathcal{T}\mathcal{T}}^S & \Sigma_{\mathcal{T}\mathcal{F}}^S \\ 0 & 0 & -C_\Gamma^\dagger & E_{\mathcal{F}}^\dagger & \Sigma_{\mathcal{F}\mathcal{T}}^S & \Sigma_{\mathcal{F}\mathcal{F}}^S \end{bmatrix} \begin{bmatrix} V_{\mathcal{T}}^F \\ P_{\mathcal{T}} \\ P_{\mathcal{F}} \\ S_{\mathcal{T}} \\ V_{\mathcal{T}}^S \\ V_{\mathcal{F}}^S \end{bmatrix} = \begin{bmatrix} 0 \\ G_{\mathcal{T}} \\ 0 \\ 0 \\ F_{\mathcal{T}} \\ 0 \end{bmatrix}$$

Numerical results

- **Verification of convergence rates on analytical solutions:**
  - ► $\mathcal{O}(h^{k+1})$ in H^1-norm
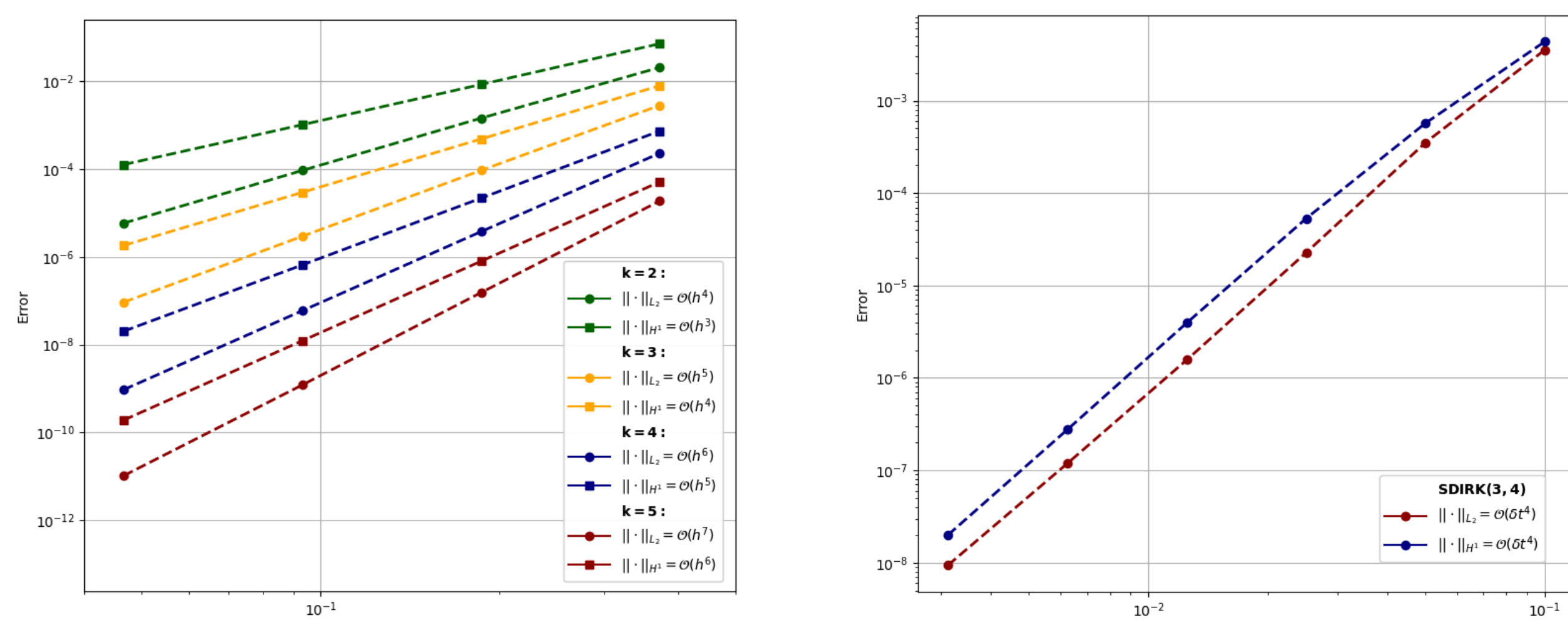 - ► $\mathcal{O}(h^{k+2})$ in L^2-norm (**superconvergence**)

Fig. 5: Left panel: Errors as a function of the mesh size with $\Delta t = 0.1 \times 2^{-5}$. Right panel: Errors as a function of the time-step with $k' = k + 1 = 6$ and dx $= 2^{-5}$.

- **Realistic test case**
  - ► **Computational domain:**
    - Acoustic region on the upper side
    - Elastic region on the lower side
  - ► **Homogeneous Dirichlet conditions**
  - ► **Intial condition:** pressure Ricker wavelet
$$p_0(x, y) := -\frac{4}{10} \sqrt{\frac{10}{3}} (1600 r^2 - 1) \pi^{-1/4} e^{-800 r^2}$$
$$v_0^F := \mathbf{0}, \quad v_0^S := \mathbf{0}, \quad \varepsilon_0 := \mathbf{0}.$$
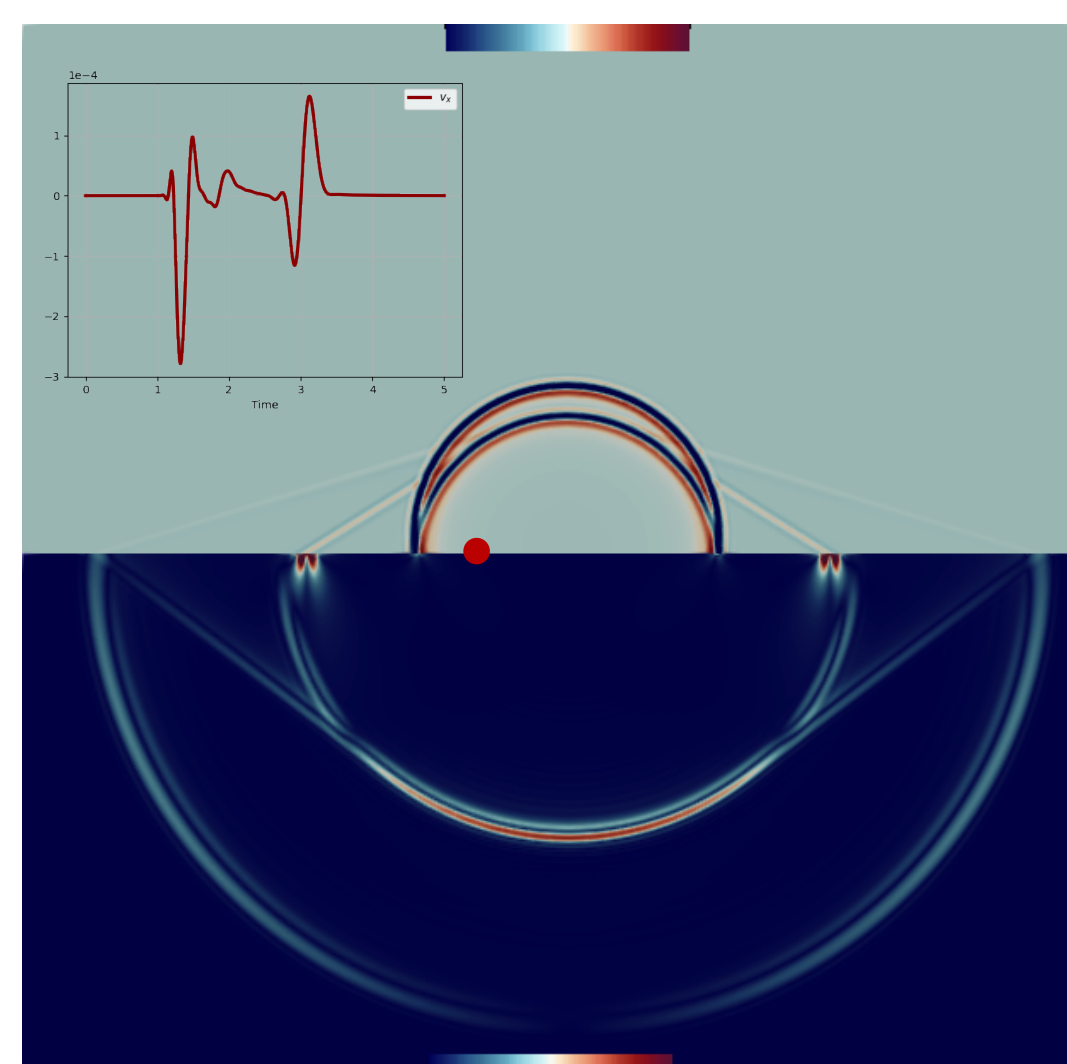 - ► **Time integration scheme:** SDIRK(s,s+1)

Fig. 6: Two-dimensional distribution of the acoustic pressure (upper side) and elastic velocity norm (lower side), predicted by the HHO-SDIRK (3, 4) at $t = 5$ s. Simulation parameters: $k' = k + 1 = 2$, dx $= 2^{-8}$ and $\Delta t = 0.1 \times 2^{-8}$.

Energy conservation of the scheme

- **Mechanical energy of the scheme:** $\mathcal{E}_h(t) := \mathcal{E}_h^S(t) + \mathcal{E}_h^F(t)$ with
$$\mathcal{E}_h^F(t) := \frac{1}{2} ||v_{\mathcal{T}}^F(t)||_{L^2(\rho_F; \Omega_F)}^2 + \frac{1}{2} ||p_{\mathcal{T}}(t)||_{L^2(\frac{1}{\kappa}; \Omega_F)}^2, \qquad \mathcal{E}_h^S(t) := \frac{1}{2} ||v_{\mathcal{T}}^S(t)||_{L^2(\rho_S; \Omega_S)}^2 + \frac{1}{2} ||\varepsilon_{\mathcal{T}}(t)||_{L^2(\mathcal{C}; \Omega_S)}^2$$

- **Semi-discrete energy conservation of the scheme**
$$\mathcal{E}_h(t) = \mathcal{E}_h(0) + \int_0^t \left[(f(\alpha), v_{\mathcal{T}}^S(\alpha))_{L^2(\Omega_S)} + (g(\alpha), p_{\mathcal{T}}(\alpha))_{L^2(\Omega_F)} - s_h^S(\hat{v}_h^S(\alpha), \hat{v}_h^S(\alpha)) - s_h^F(\hat{p}_h(\alpha), \hat{p}_h(\alpha)) \right] d\alpha$$

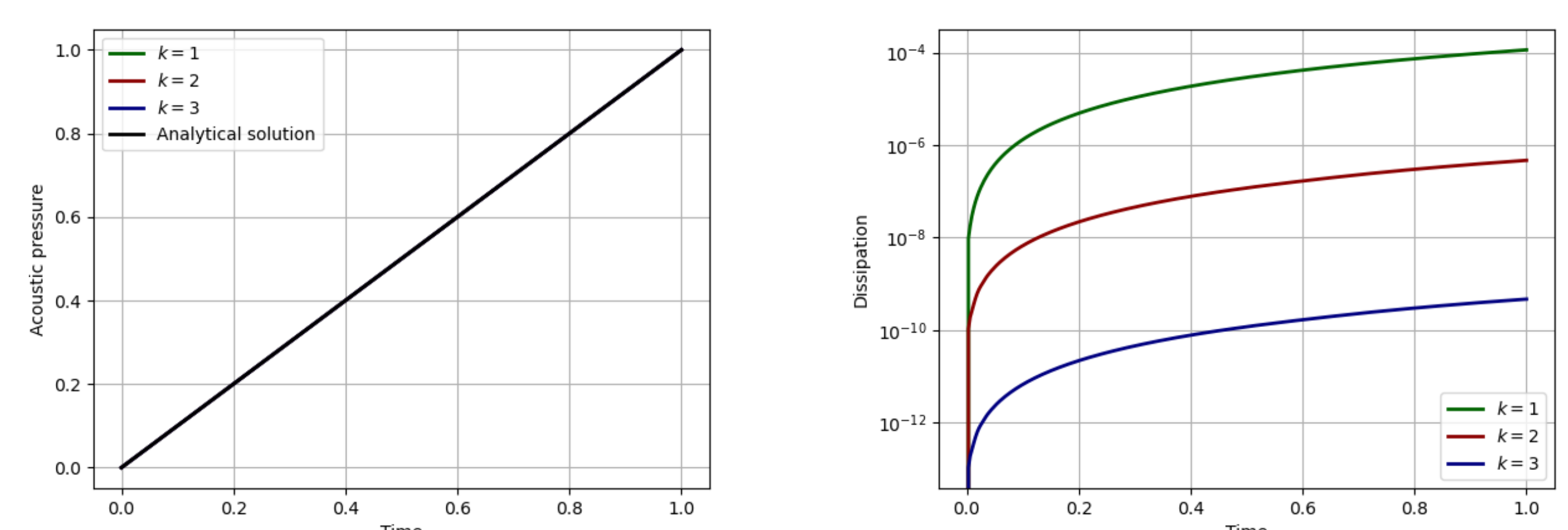- **Validation on analytic test cases**

Fig. 7: Demonstration of the negligible nature of the energy dissipation introduced by the HHO scheme.

Some references

[1] Di Pietro and Ern. "A hybrid high-order locking-free method for linear elasticity on general meshes". In: *Comput. Meth. Appl. Mech. Engrg.* 283 (2015), pp. 1–21.

[2] Burman, Duran, and Ern. "Hybrid high-order methods for the acoustic wave equation in the time domain". In: *Comm. App. Math. Comp. Sci.* 4.2 (2022), pp. 597–633.

[3] Burman, Duran, Ern, and Steins. "Convergence Analysis of Hybrid High-Order Methods for the Wave Equation". In: *J. Sci. Comput.* 87.3 (2021), p. 91.

[4] Terrana, Vilotte, and Guillot. "A spectral hybridizable discontinuous Galerkin method for elastic-acoustic wave propagation". In: *Geophys. J. Int.* 213.1 (2017), pp. 574–602.